

Absolute spectral responsivity measurements of solar cells by a hybrid optical technique

Behrang H. Hamadani,^{1,*} John Roller,¹
Brian Dougherty¹, Fiona Persaud² and Howard W Yoon³

¹Engineering Laboratory, National Institute of Standards and Technology, Gaithersburg, MD 20899, USA

²Newport Corporation, 150 Long Beach Blvd, Stratford, CT, 06615

³Physical Measurements Laboratory, National Institute of Standards and Technology, Gaithersburg, MD 20899, USA

*behrang.hamadani@nist.gov

Abstract: An irradiance mode, absolute differential spectral response measurement system for solar cells is presented. The system is based on combining the monochromator-based approach of determining the power mode spectral responsivity of cells with an LED-based measurement to construct a curve representing the light-overfilled absolute spectral response of the entire cell. This curve can be used to predict the short circuit current (I_{sc}) of the cell under the AM 1.5 standard reference spectrum. The measurement system is SI-traceable via detectors with primary calibrations linked to the NIST absolute cryogenic radiometer. An uncertainty analysis of the methodology places the relative uncertainty of the calculated I_{sc} at better than ± 0.8 %.

©2013 Optical Society of America

OCIS codes: (350.6050) ; (040.5350) ; (120.4140) ; (120.0120)

1. Introduction

The spectral responsivity (SR) measurement of solar cells – which quantifies the wavelength dependence of the cell's photocurrent generation when normalized for the input irradiance or the radiant power of the incident monochromatic radiation [1] – is a very important photovoltaic (PV) characterization technique [1,2]. The absolute determination of the SR of a solar cell, if done under appropriate conditions such as uniform overfill illumination and proper light biasing, can be used to predict the short circuit current (I_{sc}) of the device under any incident spectral irradiance, including the standard air mass 1.5 (AM 1.5) solar spectrum [3,4]. One advantage of this approach is that it provides a direct route for SI (International System of Units) traceability of the I_{sc} measurement instead of relying on the World Radiometric Reference (WRR) scale. Furthermore, having prior knowledge of the I_{sc} of the test cell during indoor or outdoor electrical performance and efficiency measurements eliminates the need to use a separate reference cell for irradiance monitoring.

The differential spectral responsivity (DSR) method [4–10] is the most widely used method for measuring the SR of a solar cell. Using this technique, a small modulated (quasi) monochromatic light beam and a more intense steady-state white light source (the light bias) simultaneously illuminate the solar cell, producing a photocurrent that is the sum of these two sources: a small ac signal superimposed on a larger dc current. The ac signal is separated, amplified and detected using a lock-in amplifier that is synced with the user-selected modulation rate of the chopped monochromatic beam. A small portion of the monochromatic beam is diverted towards a monitor photodetector in order to measure the beam's radiant

power. This radiant power, which is recorded by the same or by a separate lock-in amplifier, coupled with the cell's ac current and the monochromator's known passed wavelength, collectively define each discrete SR data point. The set of these discrete points, in turn, construct the overall SR curve. As for the radiant power of the bias light and the resulting cell dc current, their impact on the SR measurement has been described previously [5], particularly for certain types of solar cells.

The spectral responsivity measurement of a PV device can be performed in either the power mode or the irradiance mode, and each measurement can be either a relative or an absolute measurement. Power mode measurements require the knowledge of the monochromatic beam's radiant power, typically obtained using a calibrated, SI-traceable reference photodetector. For the irradiance mode, the irradiance or incident power per unit area of the monochromatic beam is required. Irradiance can be determined by fully illuminating (i.e., overfilling) a very spatially-uniform reference photodetector with the incident monochromatic radiation and then dividing the measured beam power by the aperture area of the detector. The absolute SR in power mode has SI units of $A.W^{-1}$, whereas the absolute SR in irradiance mode is reported in units of $A.m^2.W^{-1}$ [1]. With respect to these two measurement options, the more accurate and viable route for obtaining the I_{sc} of a solar cell is achieved using the irradiance mode SR curve of the cell, since the lack of spatial uniformity of the cell responsivity or presence of metal fingers on the front surface of cell can lead to systematic difference between the underfilled power responsivity measurements and the overfilled irradiance responsivity measurements.

Over the years, a variety of techniques have been adopted for achieving monochromatic illumination of the cells for the purpose of SR measurements. These include a monochromator-based approach with a broad spectrum input light source [4,7–9,11], a filter-based method with interference filters placed in front of the broad-spectrum light [5,12], using tunable laser sources [13] and using light emitting diodes (LED) [14–17]. Each technique provides a set of advantages and limitations with regard to the responsivity measurements. With regard to the monochromator method, in particular, it provides a very good wavelength range and resolution but the optical power of the output beam is typically much less than 100 μW , resulting in μA -level signals from the illuminated solar cell. The beam is also usually focused onto a small spot and hence underfills the device. Since the light bias signal (in dc form) is several orders of magnitude larger than this monochromatic source and can come from noisy sources, detection of the small modulated signal amongst the much larger and potentially noisy dc current often becomes a challenge.

An alternative to the monochromator-based approach is one that takes advantage of the relatively narrow spectral output of individual LEDs. Multi-lamp LED arrays, for example, have recently been successfully used to perform fast spectral response measurements over a wide spectral range [14–17]. The outlook and general utility of the method, moreover, continues to improve as a result of the growth and advances in solid-state lighting. The selection of high-powered LEDs at a greater variety of emission wavelengths and with narrower linewidths is slowly increasing.

Given the merits of the established monochromator-based approach and the potential for using LED sources in spectral response measurements, a hybrid spectral response system that tapped into both options was investigated. This paper summarizes the results of that effort. For this hybrid approach, the first step is to perform a power mode SR measurement using an underfilled monochromatic beam and an overfilled light bias. The beam, in this case, is created using a triple grating monochromator having a double lamp light input. The second step is to conduct an irradiance mode SR measurement using an overfilled LED quasi-

monochromatic beam and an overfilled light bias on the same test specimen. The result of the irradiance mode measurement is used as a single-wavelength scaling factor for the data obtained using the power mode measurement. The scaling yields absolute spectral responsivity data, expressed in units of $\text{A}\cdot\text{m}^2\cdot\text{W}^{-1}$, over the full bandwidth that the cell responds. From these data points, the continuous spectral response profile of the cell can be mathematically approximated and then used to estimate the short circuit current of the cell under any defined solar spectrum. Of particular interest is the short circuit current calculated when the cell is exposed to the standard AM 1.5 global tilt irradiance spectrum. This short circuit current is the key characterization parameter for reference cell calibrations and so methods that expand the ways and reduce the uncertainties for obtaining this quantity are useful to the industry.

The work to date has focused on measurements of cells with dimensions on the order of $2\text{ cm} \times 2\text{ cm}$ or less and having very good spatial uniformity. As a consequence, the shape of the spectral response curve does not change at various locations across the cell. Therefore, a single point DSR measurement works very well in scaling the (relative) spectral response data obtained using the power mode measurement.

2. Experimental Setup

A. Overall system description

The key test measurements are the cell's electrical output and the radiant power of the monochromatic light incident upon the test cell. Figures 1(a) and 1(b) show the simplified schematics of the National Institute of Standards and Technology (NIST) spectral response measurement system. With regard to the monochromator-based measurement, Figure 1(a), two different light sources, a 150 W xenon (Xe) light source and a 250 W quartz tungsten halogen (QTH) light source, supply the input radiation needed for the system's operation. The Xe source is used for the spectral range of 300 nm to 605 nm; for the spectral range $> 605\text{ nm}$, the QTH source is used. The light entering the monochromator is switched between the Xe and QTH sources using a flip mirror, which is housed in the "switch box" noted in Figure 1(a). The monochromator's output benefits from the higher radiant power and smooth spectral irradiance of the Xe source over the shorter wavelengths while avoiding the measurement errors associated with its more spiked profile at the longer wavelengths [18]. Instead, the smooth light output of the QTH source provides the monochromator's input for the noted visible-near infrared (VIS-NIR) region.

The radiation from either of the two sources is conditioned before it enters the monochromator. The light that departs the switch box, passes through a filter wheel assembly where a set of order-sorting filters ensure that higher order diffraction components are not mixed in the monochromator's output. Next, a variable-frequency mechanical chopper is employed to modulate the light at a frequency of 43 Hz. The 43 Hz frequency is chosen because it is a prime number and is sufficiently spaced away from the line frequency of 60 Hz. The modulated monochromatic light that exits the monochromator and impinges on the test cell creates a chopped current output from the cell. This chopped or alternating current (ac) output combines with the steady, direct current (dc) that is generated from simultaneously illuminating the test cell with bias lights. For light biasing, two high-powered, water-cooled white LEDs are used to fully illuminate the entire test cell. These bias lights are mounted on both sides and point directly at the PV test cell, which is mounted on the vacuum stage as shown in Fig. 1(a). These bias lights are used to ensure the cell is operating at an excitation level that is representative of daylight exposure, which is important for certain cells [4,7].

A small portion of the monochromator's light output is directed towards a sandwich Si/Ge monitor detector. The output from this detector is conditioned by a variable-gain, current-to-voltage amplifier (typically set at a gain of 10^5 V/A). This amplified voltage signal is then input to a multiplexer instrument. The solar cell's photocurrent, by comparison, is input to a variable gain transimpedance current-to-voltage preamplifier that separates the photocurrent into its dc and ac components. The dc and ac components are each fed to the multiplexer where the ac signal is measured and recorded by the lock-in amplifier while the dc signal is measured by a multimeter (not shown in Figure 1(a)). The latter measurement is particularly useful for dc-mode spectral response measurements where instead of using a light bias only a steady, monochromatic beam is used to illuminate the cell.

The instrumentation and hardware used to perform the spectral measurements has some notable features. The current preamplifier for the test solar cell, for example, is designed to handle up to 1.6 A of dc current, making it suitable for larger-area cell measurements than just the conventional 2 cm x 2 cm test cell. The multiplexer is a multi-channel input/output instrument that acts as a router for reading various signals. The multiplexer also controls the operation of the rotating mirror that is located inside the switchbox. In the original design of the system, only one lock-in amplifier was utilized; as such, the lock-in first measured the ac signal from the monitor detector preamp, followed by the cell's current preamplifier signal. A second lock-in amplifier has since been added to allow the two ac measurements to occur simultaneously rather than sequentially, thus reducing possible measurement errors. At each wavelength, the data from both lock-in amplifiers are measured for a few seconds (typically corresponding to 100 measurements) and the mean and the standard deviation are calculated and recorded for the uncertainty analysis.

The second step of the SR measurement is to use the LED-based test setup depicted in figure 1(b) to collect data that allows scaling the data collected from the monochromator-based measurements. A water-cooled LED with a centroid emission wavelength of 537.83 nm is projected towards the stage that holds the test cell. A 2 meter separation distance between the LED and the stage was found to form a large and uniform spot that completely overfills the cell and its packaging. This LED is powered using a commercial LED driver that is triggered by a function generator to supply a pulsed current. A pulse rate of 43 Hz (same as chopper's frequency) was used. White LED bias lights, powered by a constant current source, also fully and continually illuminate the cell. Using the same hardware and technique as used for the monochromator-based power-mode measurements, the cell's ac response caused by the pulsed LED is measured using the cell preamplifier (discussed above) in combination with the lock-in amplifier. Once the cell's ac photocurrent is measured, the cell is removed from the stage and a reference detector is mounted with its active plane positioned at the same *x-y-z* location as the tested cell. The detector is then illuminated by the pulsed LED light, and its response is measured. The ratio of the two measurements both conducted with their active areas overfilled and so constituting irradiance mode measurements, yields the absolute spectral responsivity of the solar cell at this one wavelength. This absolute quantity, when coupled with the power mode spectral response determined at the same wavelength using the monochromator-based method, is then used to scale all of the spectral response data from the monochromator-based, underfill, power-mode method. The end result is an absolute spectral response curve in irradiance mode for the entire response range of the cell. More details of this process follow below.

B. The monochromator

The monochromator used is a 3-grating instrument with a focal length of 260 mm. Grating #1 is used in the spectral range of 300 nm to 720 nm, while grating #2 is used in the range of 720

nm to 1540 nm. Grating #3 is used in the spectral range > 1540 nm. Wavelength calibration of the monochromator was performed using mercury, neon and krypton pen lights. The wavelength uncertainties for gratings #1 and #2, as determined from the residuals of a linear fit to the calibration data, are ± 0.5 nm and ± 0.3 nm, respectively. The monochromator wavelength linewidth for all the measurements reported here are ≈ 5 nm. The stray light measurement for the monochromator using a 395 nm LED yielded a dark/light ratio of 2.8×10^{-4} .

The radiant power profile of the monochromator's output was independently measured as part of this project. A reference silicon photodiode that is maintained and calibrated by the NIST Physical Measurement Laboratory was used for these independent measurements. This reference detector was placed 30 cm from the output port of the monochromator, the same location as the test cell during the SR measurement, and exposed to the same conditioned beam, which is approximately 1 mm in diameter. Figure 2 shows the power of the output beam when using each source, Xe and QTH. The dark dashed curve corresponds to the power delivered by the Xe source, while the red dashed curve corresponds to the power delivered by the QTH. The Xe source delivers significantly more power for wavelengths < 600 nm while showing a relatively smooth spectrum. However, for wavelengths > 700 nm, the Xe spectrum shows a significant number of spikes and large variations in output. These variations would add to the uncertainty in SR measurements and hence are avoided by switching the light source from Xe to QTH. The QTH source delivers a more constant optical output in the near infrared (NIR) range. The thick green curve in Figure 2 shows the optical power that is delivered using the dual source operation and the chosen switching value of 605 nm. This curve also reflects the design consideration to try and match the outputs of both sources, as the overall power remains relatively stable, hovering around $10 \mu\text{W}$. The small but noticeable shift in the curve at 720 nm is due to the switch between gratings #1 and #2.

C. The light bias

The light bias is operated in dc mode with a stable power supply and should be a *broad-spectrum* light source, fully illuminating the cell area. For the purpose of determining the I_{sc} under AM 1.5 conditions, the illumination intensity ideally should be close to 1000 W/m^2 . However, for solar cells whose short circuit photocurrent varies linearly with irradiance, the bias light does not need to be very intense. For the Si devices reported here, no significant nonlinearity was measured and hence the light bias current was typically between $\frac{1}{4}$ to $\frac{1}{2}$ of the I_{sc} . Even in devices where a nonlinearity with light bias intensity is observed (not reported here), an intensity level producing $1/3$ of the total 1-sun I_{sc} is usually sufficient.

The choice of the light bias source can make a significant difference on the SR measurements. SR measurements conducted at NIST using two kinds of light bias sources yielded different levels of stability and reproducibility. In one case, a 1000 W QTH light source with projection optics was used to fully illuminate the cell area, along with the normally incident monochromatic chopped beam. (The QTH lamp was positioned approximately 45 degrees off normal.) At higher light bias levels, the I_{ac} signal generated in response to the monochromatic beam, when using the previously selected 43 Hz chopping frequency, became progressively more unstable and noisy, showing large deviations at each wavelength.

A set of frequency-domain spectrum measurements were performed on the solar cell to obtain a better understanding of the I_{ac} fluctuations. The results of these measurements are shown in Figures 3(a) - 3(c) for various light bias currents. At low bias levels (typically between 0 mA to 5 mA of dc current as compared to this cell's 1-sun photocurrent of 125 mA), the noise floor at the chosen chopping frequency of 43 Hz is relatively low. As a result, the lock-in

amplifier measurements are very steady. However, as progressively larger amounts of bias irradiance are applied to the cell, significant amounts of noise, particularly at frequencies of 50 Hz or less are observed. This noise creates a major instability for the lock-in measurements and leads to larger photocurrent uncertainties. The exact mechanism(s) that creates the observed distributed noise is not definitively understood; however, the convection air currents within the lamp housing and the effect of the cooling fan are two possible contributors. It is further noted that higher frequency regions such as 130 Hz to 150 Hz or 180 Hz and above are reasonable regions for setting the chopper's mechanical frequency and SR measurements in these regions yield much better signal to noise ratios when using the QTH bias light.

In the second light bias case, two 90 W white LEDs with an irradiance spectrum reported previously [14] were mounted on water cooled plates and projection optics were used to off-axially illuminate the entire cell during the SR measurements. In contrast to the QTH light bias source, the LED operation provided very stable lock-in measurements of the photocurrent at all wavelengths. Figures 4(a) - 4(c) show the frequency-domain signal spectrum in the presence of various degrees of light bias current. Even at very high light bias levels (such as 70 mA in Fig. 4(c)), the 43 Hz monochromatic signal is not adversely affected by noise and hence this confirms the stability of the SR measurement with the lock-in amplifier. The two noise peaks at 120 Hz and 60 Hz are related to the power line frequency and its second harmonics and do not interfere with the lock-in measurements if the chopper's frequency is sufficiently spaced away from these two values. Owing to these results, the white LED lights are typically used at NIST as the source of light bias for spectral response measurements. In this way, a ratio $I_{dc} / I_{ac} \approx 2 \times 10^4$ or greater can be accommodated, thus allowing more potential range for characterizing comparatively larger cells and/or using higher levels of light bias.

D. Reference photodetector

The reference photodetector used for primary calibration of this NIST measurement system and the absolute SR measurement in irradiance mode is a solid-state transfer standard detector traceable to the absolute cryogenic radiometer maintained by NIST's Sensor Science Division. The characteristics of these detectors and various uncertainty components associated with their calibrated operation have been previously published [19]. Si and Ge standard working detectors were used to transfer the power-mode spectral responsivity to the SR system's monitor sandwich detector, in terms of a calibration factor for each wavelength. The relative combined standard uncertainty of these standard working detectors (typically 0.1 % at 550 nm) were transferred and propagated as part of the SR system's measurement uncertainty. Furthermore, a NIST reference trap detector [19] fitted with a precision aperture was used to measure the LED irradiance at the cell testing plane (in the scalar measurement). This measurement allows for a transfer of spectral irradiance scale onto our working reference photodetector which was only initially calibrated in power responsivity mode.

E. The pulsed LED projector

The pulsed green LED used for the overfill scaling measurement has an optical lens assembly to project the light uniformly onto a large spot at the measurement plane. The spot size at a distance of 2 m from the source is ≈ 66 cm in diameter and the beam divergence angle is ≈ 0.327 radians (18.75°). Figure 5(a) shows the normalized irradiance of this particular LED as measured by a spectroradiometer. The emission peak well approximates a Gaussian distribution and has a full width at half max (FWHM) linewidth of 32.7 nm. The centroid emission wavelength λ_{cent} of the LED, given by:

$$\lambda_{\text{cent}} = \frac{\int \lambda \cdot E_{\text{LED}}(\lambda) d\lambda}{\int E_{\text{LED}}(\lambda) d\lambda} \quad (1)$$

is 537.83 nm, where $E_{\text{LED}}(\lambda)$ is the LED irradiance. It was determined that if the LED is temperature stabilized and operated with a stable pulsed current, its irradiance temporal profile yields a relative standard deviation of less than 0.03 % over a 30 min period, as shown in Fig. 5(b). This superior stability is important because the absolute spectral responsivity using the irradiance mode requires two consecutive measurements at the same xyz location: one for the reference photodetector current (for the irradiance determination) and one for the solar cell current. This stability ensures a very small error associated with this substitution.

The irradiance uniformity within the measurement test plane is as important as temporal stability. To measure the nonuniformity down to the mm scale, a 1 mm aperture was placed on a photodetector and moved over an area of $2 \text{ cm} \times 2 \text{ cm}$, corresponding to the area of the largest solar cells reported in this work. This uniformity map is shown in Figure 6. A relative standard deviation of 0.63 % was observed over this entire area, thus demonstrating a very good uniformity. However, since the reference photodetector used for evaluating the test plane irradiance has a much larger active area of 1.036 cm^2 with a negligible spatial nonuniformity, the irradiance variation over the full 4 cm^2 area only amounts to about 0.12 % by comparing the mean irradiance over a 1 cm^2 area with the mean value over a 4 cm^2 area. This percentage is used in the uncertainty analysis associated with illumination nonuniformity in the test plane.

3. SR Calculations, Results and Discussion

A. Methodology

The calibration data ($R_s(\lambda)$ vs λ , where R_s is the standard detector responsivity) associated with the NIST reference photodetector are transferred onto the monitor Si/Ge sandwich detector in terms of a transfer calibration value, $C_{\text{tr}}(\lambda)$ given by:

$$C_{\text{tr}}(\lambda) = \frac{R_s(\lambda)}{2.221 G (V_s(\lambda)/V_m(\lambda))} \quad (2)$$

where $V_m(\lambda)$ is the voltage signal measured from the monitor detector and $V_s(\lambda)$ is the signal recorded from the reference detector during the calibration procedure. The gain factor G is defined as $G = G_m / G_{\text{DUT}}$, where G_m is the monitor photodetector's preamplifier gain (typically set at 10^5 V/A) and G_{DUT} is the amplifier's gain for device under test. For calibration purposes, G_{DUT} is the gain setting used to record the reference detector output, V_s . The numerical factor of 2.221 is used to allow for conversion of root-mean-square (RMS) signal values recorded by the lock-in amplifier to peak-to-peak values because lock-ins measure the first Fourier (sine) component of the input signal which in this case is a square wave, and the standard detector responsivity is measured in dc mode. Once the calibration transfer from the reference photodetector onto the monitor detector is accomplished, the system is ready to measure the spectral response of solar cells.

The responsivity of a test cell, $R_t(\lambda)$, is given by:

$$R_{\text{t, pwr mode}}(\lambda) = 2.221 C_{\text{tr}}(\lambda) G (V_t(\lambda)/V_m(\lambda)) \quad (3)$$

where $V_t(\lambda)$ is the voltage signal from the cell under test. If the same detector and device gain settings are used for both the calibration of the system and subsequent device measurements, the gain value drops out during $R_t(\lambda)$ measurements, hence eliminating one component of uncertainty in the overall measurement. Equation 3 determines the spectral responsivity of a test cell in the underfill illumination mode (power mode), as the beam size is small. These $R_t(\lambda)$ values, reported in units of A/W, cannot be used to calculate the short circuit current of the solar cell because they do not represent the responsivity of the whole cell. However, these responsivity curves can be used to calculate a spectral mismatch factor, or can be reported in relative units to give an idea of the shape and range of the cell's solar responsivity.

The solar cell's absolute spectral responsivity for irradiance mode at a specified wavelength is obtained by measuring the short circuit current of the test cell at a certain test plane, followed by substitution and measurement of the short circuit current of the reference photodetector. As noted previously, the entire solar cell area is fully illuminated by the LED spotlight. The spectral response of the solar cell at the LED emission wavelength of $\lambda_{\text{cent}} = 537.83$ nm is then given by:

$$R_{t, \text{irrd mode}}(\lambda_{\text{cent}}) = \frac{(V_t/G_t)}{(V_s/G_s)} \cdot R_s^* \cdot A \quad (4)$$

V_t and V_s are voltage signal measurements of the test cell and the reference detector, G_t and G_s are the test cell and the detector gain settings, respectively and A is the effective detector area. R_s^* is the effective spectral responsivity for the reference detector, subjected to LED illumination, defined as:

$$R_s^*(\lambda_{\text{cent}}) = \frac{\int R_s(\lambda) \cdot E_{\text{LED}}(\lambda) d\lambda}{\int E_{\text{LED}}(\lambda) d\lambda} \quad (5)$$

to accounts for the fact that the detector sees a quasi-monochromatic (as opposed to a true monochromatic) beam of light. $R_{t, \text{irrd mode}}$ has a unit of $\text{A} \cdot \text{m}^2 \cdot \text{W}^{-1}$.

With the absolute SR in irradiance mode at $\lambda = \lambda_{\text{cent}}$ is known, the absolute spectral response at all wavelengths in irradiance mode is calculated from:

$$R_{t, \text{irrd mode}}(\lambda) = SF(\lambda_{\text{cent}}) \cdot R_{t, \text{pwr mode}}(\lambda) \quad (6)$$

where $SF(\lambda_{\text{cent}}) = R_{t, \text{irrd mode}}(\lambda_{\text{cent}})/R_{t, \text{pwr mode}}(\lambda_{\text{cent}})$ is the scale factor from the LED measurement and allows for the construction of the entire SR curve in irradiance mode.

With the absolute spectral responsivity for irradiance known, the short circuit current of the solar cell can be calculated under any illumination conditions. For example, the I_{sc} predicted when the cell is subjected to an AM 1.5 global tilt spectrum [20] is given by:

$$I_{\text{sc}} = \int R_{t, \text{irrd mode}}(\lambda) \cdot E_{\text{AM1.5}}(\lambda) d\lambda \quad (7)$$

where $E_{\text{AM1.5}}(\lambda)$ is the spectral irradiance associated with AM 1.5 global tilt conditions. It is noted that the area of the solar cell (or device under test) plays no role in the calculation above and hence does not need to be determined beforehand.

B. Spectral response measurement results

In Figures 7(a)-7(c), the spectral responsivity in power mode for a reference Si solar cell ($2 \text{ cm} \times 2 \text{ cm}$) is shown for the cases of no light bias, with QTH light bias, and with white LED

light bias, respectively. As discussed extensively in section 2C, the QTH source introduces a significant amount of noise in the lock-in measurements (here at 43 Hz chopping frequency) and hence the standard deviations (error bars) are relatively large. However, the white LED light bias allows for a smooth and low-noise measurement of the ac current generated in the cell. For most of the monocrystalline Si cells tested, the effect of the level of light bias was small and the shape of the SR curve did not depend on the spectral shape of the light bias used. Therefore, a white LED bias source was determined to be a perfectly permissible source for providing bias illumination.

So far, the procedure of scaling the underfilled SR data obtained from the power-mode measurements with the result from the irradiance mode measurement has been completed on three mono-silicon solar cells. Each of these cells was obtained from a different source. Two of the cells have similar construction: glass fronts and a 2 cm x 2 cm wafer size. The third cell has a KG5-filtered front and a circular cell area of 0.076 cm². The SR results for these three different solar cells are shown in Figure 8. The y-axis responsivities are plotted in units of A.m².W⁻¹ and therefore are cell size-dependent. For ease of comparison, the curves for two 4 cm² cells are plotted against the left y-axis and the curve for the smallest cell is plotted against the right y-axis.

C. Measurement uncertainty

The combined uncertainty (at each wavelength) of the absolute spectral response curves (shown in Fig. 8) include a variety of type A (uncertainties associated with repeated measurements) and type B (uncertainties associated with various other sources) uncertainties. The most important ones are the primary reference detector calibration uncertainty of $\pm 0.1\%$ (at 540 nm), wavelength calibrations uncertainties of $\pm 0.046\%$, detector area uncertainty of $\pm 0.21\%$, illumination nonuniformity errors of $\pm 0.11\%$, and a distance measurement uncertainty of $\pm 0.07\%$. Other uncertainties such as reproducibility and repeatability, raw data's standard deviations, errors associated with calibration transfers from the reference diode onto the monitor diode, etc, were also considered and included in the analysis.

Figure 9 shows the relative combined $k=1$ standard uncertainty of the spectral response curve associated with reference Si cell #1. The increased uncertainties at the two ends of the spectral range are mostly due to the primary detector's uncertainties. They do not affect the overall I_{sc} uncertainty appreciably because the spectral responsivity values drop substantially in these outer ranges and so minimally contribute to the uncertainty in the overall I_{sc} value. The combined uncertainty for I_{sc} is obtained by first calculating the curves for the upper and the lower bounds of the product of responsivity and AM 1.5 irradiance (from the combined standard uncertainty at each wavelength), followed by calculating the integral of each curve which yield the lower and upper bounds of the I_{sc} . This procedure assumes a lack of correlation between each spectral responsivity data point. For the cells tested thus far, the representative relative expanded uncertainty ($k=2$) for I_{sc} is $\pm 0.76\%$. Comparing this finding with other PV testing laboratories, it is noted that secondary certifying labs typically report $k=2$ uncertainties of $\pm 1.4\%$, while primary laboratories such as the National Renewable Energy Laboratory (NREL), the National metrology Center in Singapore and the Physikalisch-Technische Bundesanstalt (PTB) in Germany have reported uncertainties of $\pm 0.9\%$, $\pm 1\%$, $\pm 0.5\%$ respectively [8–10].

D. I_{sc} determination and inter-laboratory comparisons

The short circuit currents of the two reference Si cells shown in Fig. 8 were computed using Eq. 7 and compared with the values reported in the original calibration certificate supplied by

a certified testing laboratory. The third cell, having the ID “US1”, is a primary reference cell that is maintained by NREL. In the case of this US1 cell, NIST completed its two-step SR measurements and shared the resulting I_{sc} with NREL in advance of learning the I_{sc} as measured by NREL. The summary of these comparisons is shown in Table 1. Excellent agreement is observed between the NIST measurements and the certified values for all three cells. With regard to the direct inter-comparison with NREL in particular, the two I_{sc} values differ by only 0.21 %, which is well within the uncertainty window. These findings support the use of the described two-step SR measurement methodology for determining the spectral response and the short circuit current for these and likely other types of solar cells.

4. Conclusions

Absolute differential spectral responsivity measurements for irradiance mode of Si-based solar cells with dimensions up to 2 cm x 2 cm have been demonstrated using the traditional monochromator-based technique combined with a pulsed LED method. The monochromator approach with an input dual light source and a stable white LED source for light bias is used to obtain power mode spectral response curves. A pulsed green LED source projected over a large distance onto the solar cell combined with an LED light bias source is then used to determine a single wavelength absolute spectral responsivity via an irradiance mode measurement. This single wavelength value serves as a scaling factor for constructing the overall absolute spectral response of the cell in irradiance mode. The short circuit current of three solar cells for AM 1.5 global tilt conditions were calculated from these spectral response curves. These short circuit currents show excellent agreement with other laboratory calibrations that use a different measurement approach and/or a different traceability path.

Acknowledgement

We thank Jeanne Houston and George Eppeldauer for supplying the calibrated Si and Ge photodiodes used in our laboratory. We thank Keith Lykke for the loan of the trap detector, and Toni Litorja for the aperture area measurements. We are grateful to Domenic Assalone of Newport Corporation for closely supervising the engineering work on the monochromator system. Finally, we are deeply indebted to Dr. Keith Emery of NREL for arranging the inter-laboratory comparison and useful discussions.

References and links

1. "Standard test method for spectral responsivity measurements of photovoltaic devices," ASTM Standard E1021-06 **12.02**, 500–509 (2009).
2. K. L. Chopra and S. R. Das, *Thin Film Solar Cells* (Plenum, 1983).
3. J. L. Shay, S. Wagner, R. W. Epworth, K. J. Bachmann, and E. Buehler, "A simple measurement of absolute solar-cell efficiency," *J. Appl. Phys* **48**, 4853–4855 (1977).
4. S. Winter, T. Wittchen, and J. Metzdorf, "Primary reference cell calibration at the PTB based on an improved DSR facility," *Proc. 16th European Photovoltaic Solar Energy Conf.* 1–4 (2000).
5. L. Boivin, W. Budde, C. Dodd, and S. Das, "Spectral response measurement apparatus for large area solar cells," *Appl. Opt.* **25**, 2715–2719 (1986).
6. J. S. Hartman and M. A. Lind, "Spectral response measurements for solar cells," *Solar Cells* **7**, 147–157 (1982).

7. J. Metzdorf, "Calibration of solar cells. 1: The differential spectral responsivity method.," *Appl. Opt.* **26**, 1701–1708 (1987).
8. J. Metzdorf, S. Winter, and T. Wittchen, "Radiometry in photovoltaics: calibration of reference solar cells and evaluation of reference values," *Metrologia* **37**, 573–578 (2000).
9. G. Xu and X. Huang, "Primary Calibration of Solar Photovoltaic Cells At the National Metrology Centre of Singapore," *Energy Procedia* **25**, 70–75 (2012).
10. K. Emery, "Photovoltaic Efficiency Measurements," *Proc. SPIE* **5520**, 36–44 (2004).
11. R. Ciocan, Z. Li, D. Han, D. Assalone, F. Yang, T. Bilir, E. Ciocan, and K. Emery, "A fully automated system for local spectral characterization of photovoltaic structures," *PVSC 35th IEEE*, 1675–1677 (2010).
12. S. Silvestre, L. Sentis, and L. Castaner, "A fast low-cost solar cell spectral response measurement system with accuracy indicator," *IEEE Trans. Instrum. Meas.* **48**, 944–948 (1999).
13. S. W. Brown, G. P. Eppeldauer, and K. R. Lykke, "Facility for spectral irradiance and radiance responsivity calibrations using uniform sources," *Appl. Opt.* **45**, 8218–8237 (2006).
14. B. H. Hamadani, J. Roller, B. Dougherty, and H. W. Yoon, "Versatile light-emitting-diode-based spectral response measurement system for photovoltaic device characterization.," *Appl. Opt.* **51**, 4469–76 (2012).
15. F. C. Krebs, K. O. Sylvester-Hvid, and M. Jørgensen, "A self-calibrating led-based solar test platform," *Prog. Photovolt: Res. Appl.* **19**, 97–112 (2011).
16. G. Zaid, S.-N. Park, S. Park, and D.-H. Lee, "Differential spectral responsivity measurement of photovoltaic detectors with a light-emitting-diode-based integrating sphere source.," *Appl. Opt.* **49**, 6772–83 (2010).
17. J. A. Rodríguez, M. Fortes, C. Alberte, M. Vetter, and J. Andreu, "Development of a very fast spectral response measurement system for analysis of hydrogenated amorphous silicon solar cells and modules," *Materials Science and Engineering: B* **178**, 94–98 (2013).
18. H. Field, "Solar cell spectral response measurement errors related to spectral band width and chopped light waveform," *PVSC 26th IEEE*, 471–474 (1997).
19. T. C. Larason and J. M. Houston, "Spectroradiometric detector measurements: ultraviolet, visible, and near-infrared detectors for spectral power," *NIST Special Publication* **250-41**, (2008).
20. "Standard tables for reference solar spectral irradiances: Direct normal and hemispherical on 37 degrees tilted surface," *ASTM Standard G173-03* (2012).
21. "Certain commercial equipment, instruments, or materials are identified in this paper to foster understanding. Such identification does not imply recommendation or endorsement by the National Institute of Standards and Technology, nor does it imply that the materials or equipment identified are necessarily the best available for the purpose" .

Cell ID	I_{sc} [NIST measurement]	Certification Laboratory [21]	I_{sc} [Certification Laboratory]	Percent Difference
VLSI10510-0193	125.03 ± 0.92 mA	VLSI Standards	125.6 ± 1.8 mA	0.45 %
VLSI10540-0144	134.2 ± 1.02 mA	VLSI Standards	134.3 ± 1.9 mA	0.074 %
US1	10.02 ± 0.076 mA	NREL	9.9985 ± 0.09099 mA	0.21 %

Table 1: The NIST-determined short circuit currents of a few reference solar cells using the absolute differential spectral response method and the comparison of these values with other laboratories. The uncertainty values are reported at the 95 % confidence interval.

Figure Captions

Figure 1: (a) The overview of the monochromator-based power mode spectral response measurement system (b) Schematic of the one-point irradiance mode spectral response measurement.

Figure 2: The radiant power of the monochromator's output with just the Xe source as the input light (long dashed line), the QTH light source only (short dashed lines), and both sources during a normal measurement run where the Xe source is used for all $\lambda < 605$ nm, and QTH is used for all $\lambda > 605$ nm (thick continuous line).

Figure 3: The frequency-domain signal spectra (10 Hz – 200 Hz) of a solar cell illuminated by a 43 Hz chopped monochromatic beam and various amounts of light bias illumination provided by a QTH light source. The signal is measured as V_{rms} across a 50 Ω -shunted termination. The background noise is significantly higher for larger amounts of bias illumination.

Figure 4: The frequency-domain signal spectra (10 Hz – 200 Hz) of a solar cell illuminated by a 43 Hz chopped monochromatic beam and various amounts of light bias illumination provided by a white LED light sources. The background noise remains unchanged for large amounts of bias illumination. The two large peaks are related to the power line frequency.

Figure 5: (a) Normalized irradiance of our pulsed green LED projector as measured by a spectroradiometer. (b) Excellent temporal stability of this LED operated in pulse mode, over a period of 30 min.

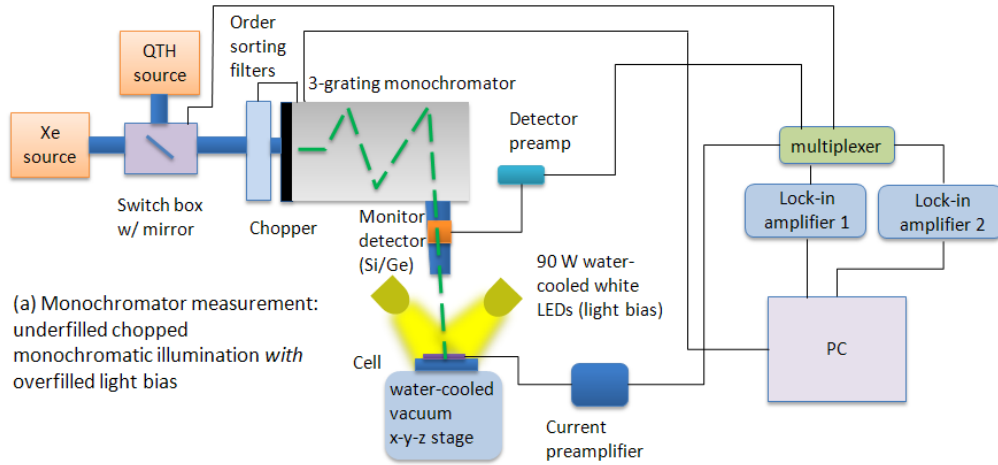
Figure 6: Illumination uniformity map produced by the pulsed green LED at the measurement plane, mapped over an area of 2 cm by 2 cm. The detector aperture was 1 mm in size.

Figure 7: The spectral responsivity in power mode for a reference Si solar cell (2 cm \times 2 cm) with (a) no light bias, (b) QTH light bias, and (c) the white LED light bias. The white LED light bias source is very stable and therefore the lock-in amplifier provides raw signals with much lower standard deviations than with the QTH source.

Figure 8: The irradiance mode spectral responsivity curves for 3 solar cells obtained according to the methodology outlined in section 3A.

Figure 9: Relative combined $k=1$ standard uncertainty of the spectral response curve associated with reference Si cell #1.

Figure 1



(b) Single or multi-point measurement: Overfilled pulsed LED monochromatic illumination *with* overfilled light bias

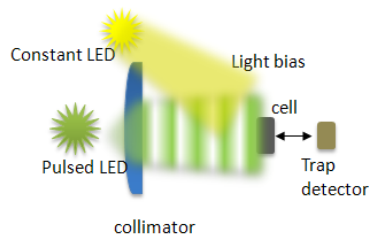


Figure 2

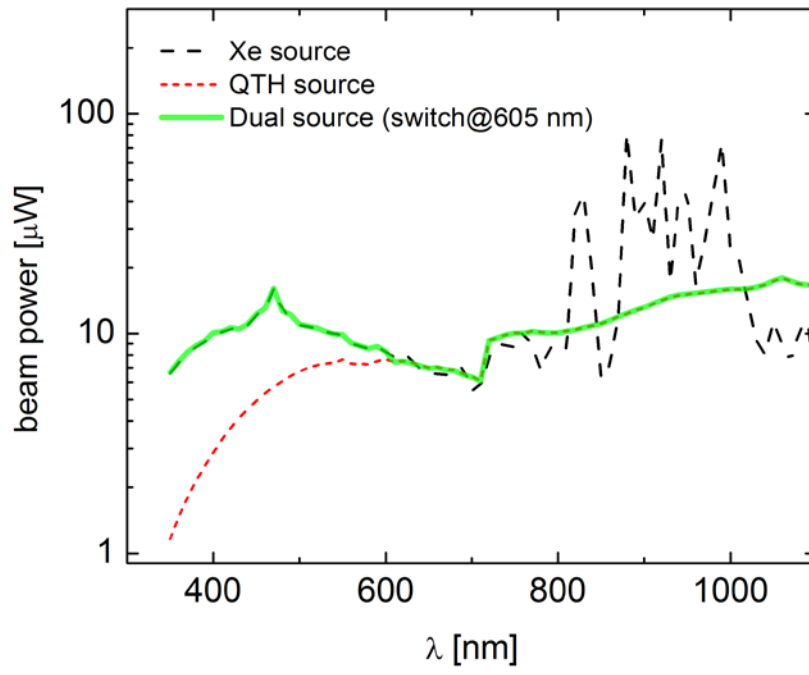


Figure 3

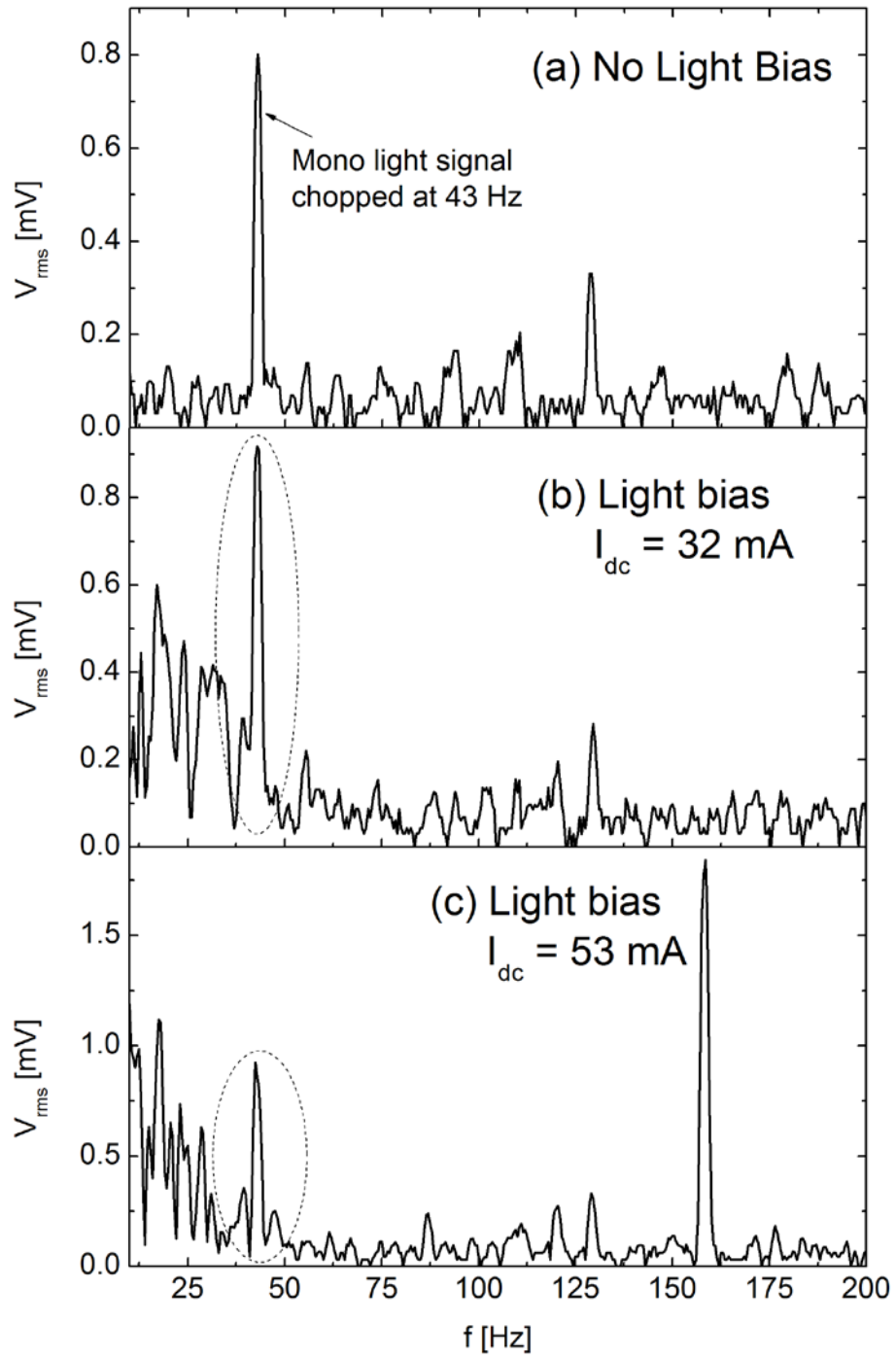


Figure 4

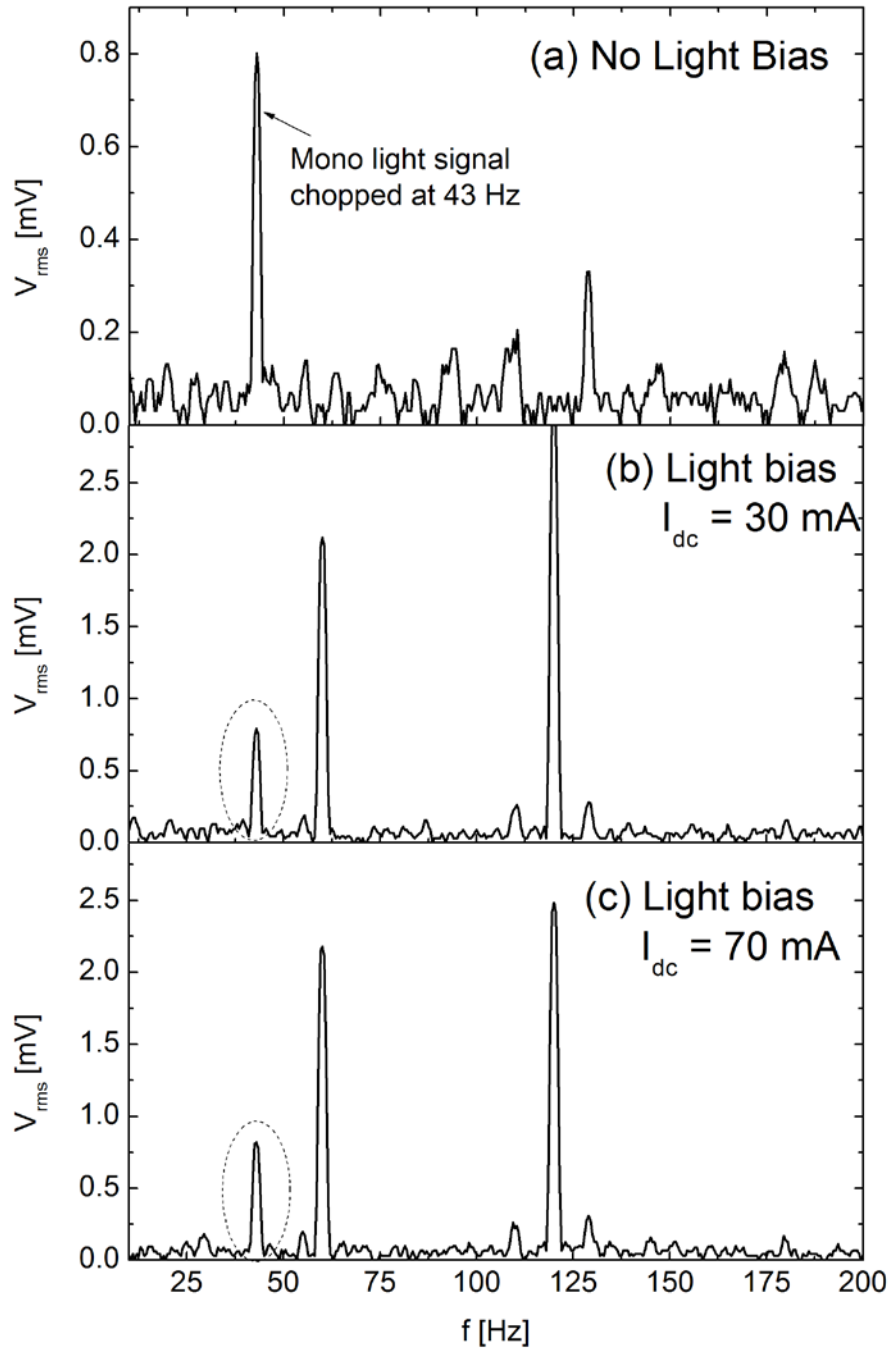


Figure 5

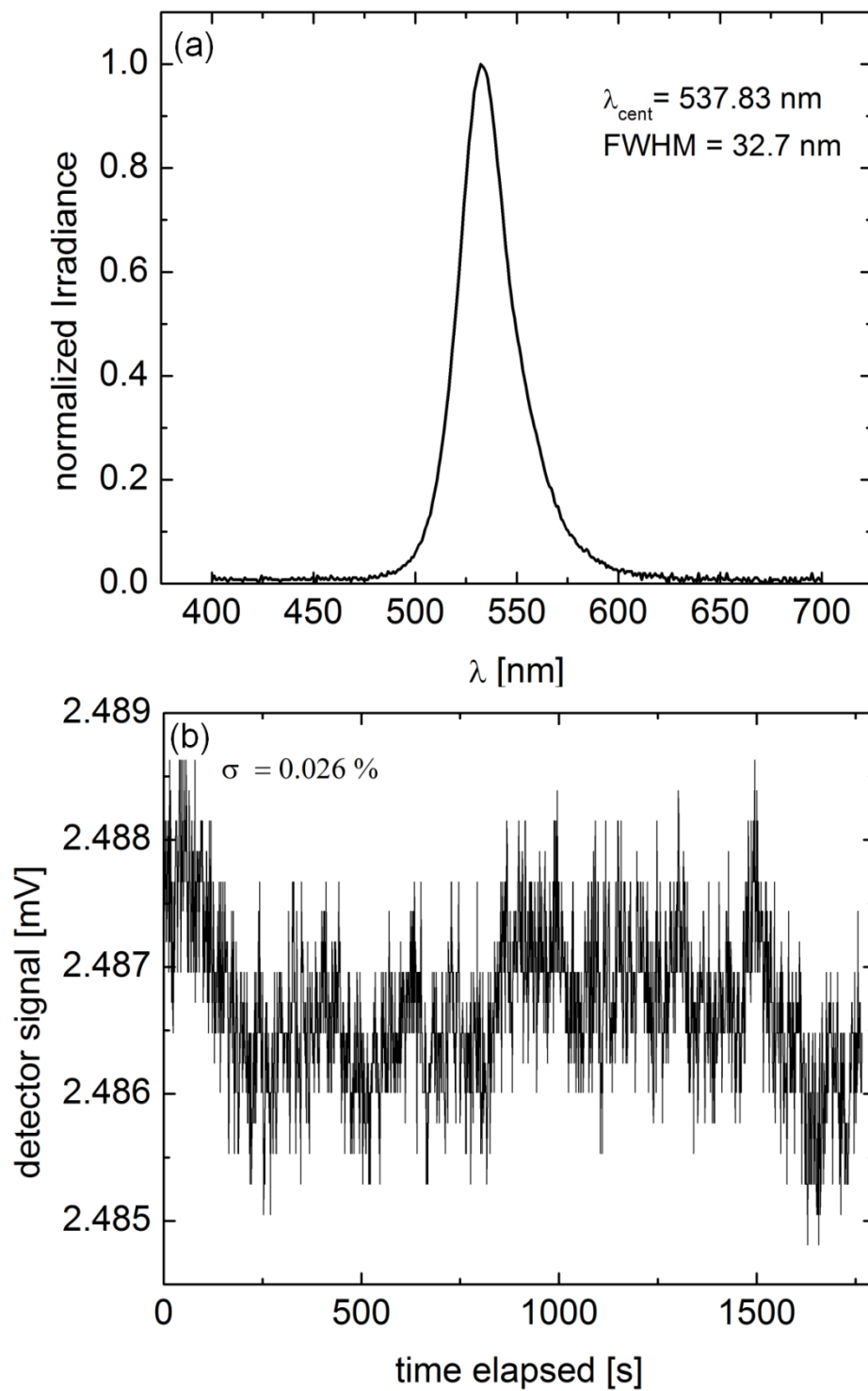


Figure 6

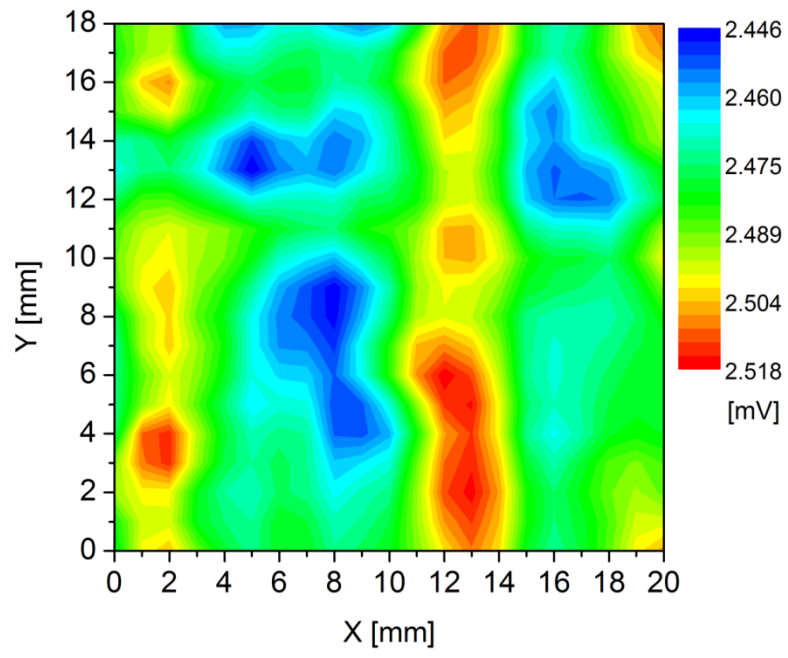


Figure 7

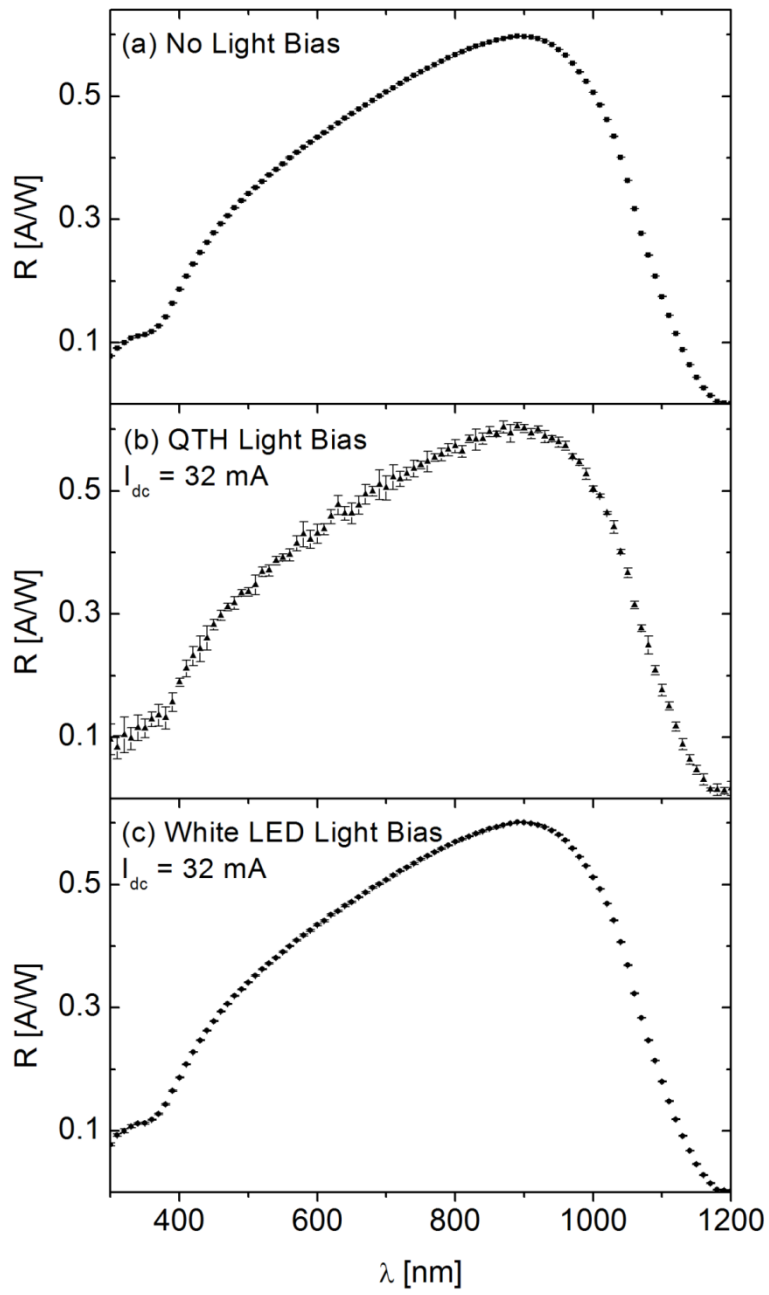


Figure 8

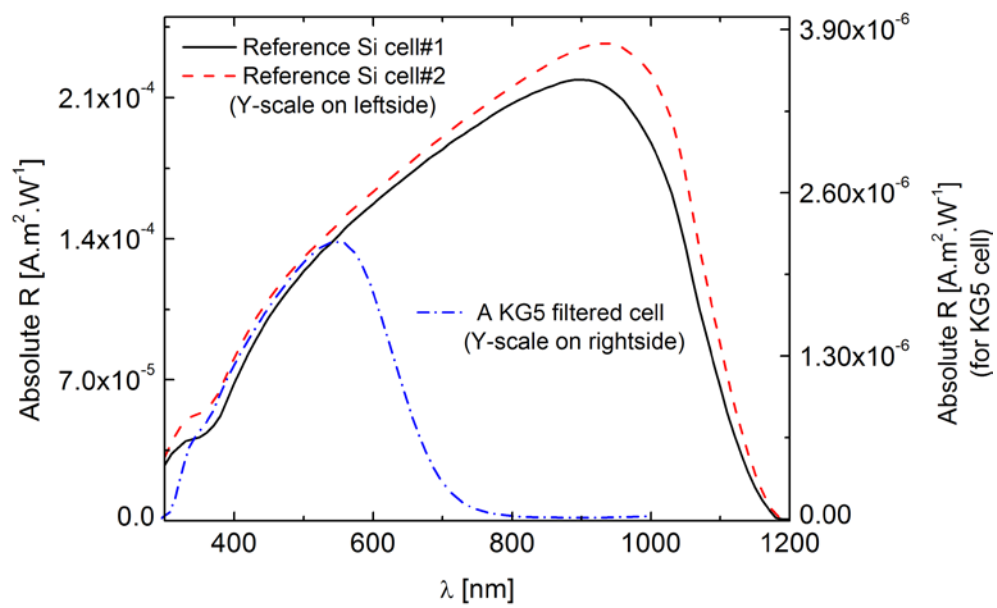


Figure 9

